Journal of Atmospheric and Solar-Terrestrial Physics 73 (2011) 1454–1459

Contents lists available at ScienceDirect

Journal of Atmospheric and Solar-Terrestrial Physics

journal homepage: www.elsevier.com/locate/jastp

Statistical studies of geomagnetic storms with peak $Dst \leq -50$ nT from 1957 to 2008

E. Echer [a,*], W.D. Gonzalez [a], B.T. Tsurutani [a,b]

[a] INPE, São José dos Campos, SP, Brazil
[b] Jet Propulsion Lab, Pasadena, CA, USA

ARTICLE INFO

Article history:
Received 25 March 2010
Received in revised form
31 March 2011
Accepted 10 April 2011
Available online 6 May 2011

Keywords:
Geomagnetic storms
Ring current
Magnetosphere
Space weather

ABSTRACT

A catalog of 1377 geomagnetic storms with peak Dst (Dst_p) ≤ -50 nT for the period 1957–2008 has been compiled. The dependence of Dst_p on the solar cycle and annual variation are studied in this paper. It is found that geomagnetic storm peak intensity distribution can be described by an exponential form, $P(Dst_p) \approx 1.2e^{-Dst_p/34}$, where P is the probability of geomagnetic storm occurrence with a given value Dst_p. The updated solar cycle and annual distribution of geomagnetic storms have confirmed the expected behavior. For the solar cycle variation, geomagnetic storms display a two-peak distribution, with one peak close to solar maximum and the other a few years later in the beginning of the declining phase. Geomagnetic storms follow the well-known seasonal variation of geomagnetic activity. More intense storms show a peak in probability occurrence in July, confirming previous observations. These results are of practical importance for space weather applications.

1. Introduction

Geomagnetic storms are disturbances in the geomagnetic field and in the magnetosphere that have been studied for more than 200 years (e.g. von Humboldt 1808; Chapman and Bartels, 1940; Rostoker and Falthammar 1967; Gonzalez and Tsurutani, 1987; Gonzalez et al., 1994, 2007; Tsurutani et al., 1988, 1997, 2006a, 2006b; Echer and Gonzalez, 2004; Gonzalez and Echer, 2005; Guarnieri et al., 2006; Echer et al., 2005a, 2008). Geomagnetic storms are usually defined by ground-based, low-latitude geomagnetic field horizontal component (H) variations. The magnetic variations are proxies (and indirect measures) for disturbances in the plasma populations and current systems present in the magnetosphere (Dessler and Parker, 1959; Sckopke, 1966). It is well known that the primary interplanetary cause of geomagnetic storms is the presence of a southward interplanetary magnetic field structure in the solar wind (Rostoker and Falthammar 1967; Hirshberg and Colburn, 1969; Gonzalez and Tsurutani 1987; Tsurutani and Gonzalez, 1987; Tsurutani et al., 1988; Gonzalez et al. 1994, 1994; Echer et al., 2005a, 2005b). This magnetic field orientation allows magnetic reconnection (Dungey, 1961; Gonzalez and Mozer, 1974; Akasofu, 1981) and energy transfer from the solar wind to the Earth's magnetosphere.

Geomagnetic storms are characterized by enhanced particle fluxes in the radiation belts. These enhanced fluxes can be indirectly measured by decreases in the Earth's magnetic field horizontal component caused by the diamagnetic effect generated by the azimuthal circulation of the ring current particles. A standard measure of this is the Dst index, which is approximately proportional to the total kinetic energy of 20–200 keV particles flowing westwardly (as viewed from the northern hemisphere) in the region of ~2–6 terrestrial radii (R_E), during the storm main and recovery phases. The inner edge of the ring current is located at $4R_E$ or less from the Earth's surface during intense storms. For lesser intensity storms, the ring current is located further away from the Earth (Gonzalez et al., 1994; Daglis and Thorne, 1999; Echer et al., 2005a). The Dst index has been available since 1957 (Sugiura, 1964; Rostoker, 1972). The index primarily indicates the effects of the ring current in the geomagnetic field. One should note that the Dst index has contributions from other current systems such as the Chapman–Ferraro magnetopause current and the magnetotail current (Baumjohann, 1986; Gonzalez et al., 1994; Feldstein et al., 2003) as well. However the exact level of the various contributions is being debated (Feldstein et al., 1990, 2003). The Dst index is derived from hourly averages of the horizontal component of the geomagnetic field, usually recorded at four or six low-latitude observatories. Dst is the average of the H fields after the average solar quiet variation and the permanent magnetic field have been subtracted from the disturbed one (Sugiura, 1964). The storm recovery phase is characterized by a decay of the ring current due

* Corresponding author.
E-mail address: ezequiel.echer@gmail.com (E. Echer).

1364-6826/$ - see front matter © 2011 Elsevier Ltd. All rights reserved.
doi:10.1016/j.jastp.2011.04.021

to a combination of several different energetic particle loss mechanisms (Gonzalez et al., 1994; 1999; Fok et al., 1995; Kozyra et al., 1997). However for corotating interaction region (CIR)-caused storms, the storm recovery-phases can be somewhat deceptive. There is often fresh energy injection into the outer regions of the magnetosphere ($L > 4$, Sorras et al., 2004) in the form of high-intensity, long-duration, continuous *AE* Activity (HILDCAA) events (Tsurutani and Gonzalez, 1987; Tsurutani et al., 1995, 2006a, 2006b). For more details on the *Dst* index we refer the reader to Sugiura (1964) and Rostoker (1972).

The solar cycle dependence of storm occurrence has been previously studied, with a resultant dual peak in the occurrence frequency. One peak is found near the sunspot maximum and other in the early descending phase (Gonzalez et al., 1990, 2007; Echer et al., 2008). This is usually attributed to the solar cycle dependence of solar wind structures, with storms close to solar maximum caused by the remnants of CMEs (ICMEs), and in the descending phase by ICMEs and CIRS, (e.g, Gonzalez et al., 1999, 2007; Alves et al., 2006; Guarnieri et al., 2006; Echer et al., 2005a, 2005b, 2006, 2008; Tsurutani et al., 2006a, 2006b, 2008).

There is a well known seasonal variation in the magnetic storms with two occurrence peaks around the equinoxes. These have been attributed to axial, equinoctial and Russell–McPherron mechanisms (Priester and Catanni, 1962; Russell and McPherron, 1973; Gonzalez et al., 1994). However, Mursula et al. (2011) have shown evidence that substorms and geomagnetic activity characterized by the *Ap* index exhibit only one seasonal peak per year, giving an annual equinoctial peak. Another annual variation found in past studies (Clua de Gonzalez et al., 2001, 2002) is a peak near July. This peak occurrence is for more intense geomagnetic intense activity only.

The distribution of geomagnetic storms throughout the solar cycle and during the calendar year is a very important topic in space weather. Both scientific research and technological operations cannot be planned without this knowledge. In this work a catalog of magnetic storms during 1957–2008 is compiled. Storms with peak values of $Dst \leq -50$ nT were selected. An exponential fit function for the entire storm distribution is presented that may be useful for space weather applications. This distribution is a new result and provides the occurrence probability of a storm of a given intensity, which can be used for space weather and modeling results. Further, using this list of storms, an analysis is performed on the storm solar cycle and semi-annual/annual dependences, updating results published elsewhere in the literature (e.g, Gonzalez et al., 1990; Clua de Gonzalez et al., 2001, 2002; Echer et al., 2008).

2. Method of analysis

A list of geomagnetic storms occurred during 1957–2008 was compiled using the *Dst* data from the World Data Center for Geomagnetism—Kyoto (swdcwww.kugi.kyoto-u.ac.jp). Hourly average plots and data were carefully checked by eye and storms with peak $Dst \leq -50$ nT were selected. A total of 1377 storms were identified. Each storm profile was analyzed to separate individual storms from complex events. A full Table with dates, times of peak *Dst* and peak *Dst* values (Dst_p) for all the storms is available on request from the authors. Fig. 1 shows an example how the information from a geomagnetic storm was prepared. The storm initial, main and recovery phases, as well as the storm Dst_p, are identified and indicated in this figure. This storm occurred from 4 to 5 November 2003. This is a single step storm, so the main phase is easily identified. When storms have multiple dips, the main phase is defined starting at the end of the storm initial phase when *Dst* begins to decrease, ending at the largest

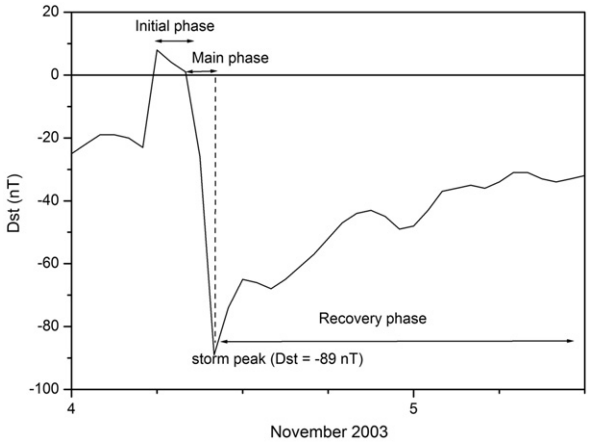

Fig. 1. Example of a geomagnetic storm (4 to 5 November 2003) identified in this study. The initial, main and recovery phases, as well as the storm peak intensity are identified in the Figure. This storm had a peak *Dst* Dst_p of −89 nT at 1000 UT, 04 November 2003.

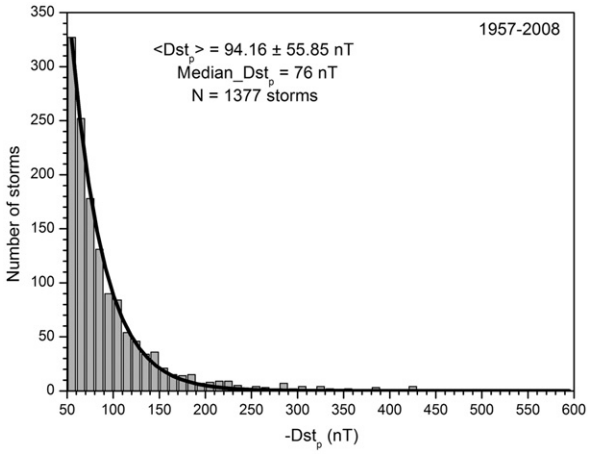

Fig. 2. Histogram of the peak *Dst* (Dst_p) for all storms (bars) and exponential fit (solid line).

negative value of *Dst* (Dst_p). When there are further dips after the peak *Dst* (but are more positive than the peak Dst_p) these are not considered as separate storms, but as part of the recovery phase. If there are more negative dips, these are considered second (third, etc.) storms.

Sunspot number annual averages from the Sunspot Index Data Center (http://www.sidc.oma.be) were used for the purpose of identifying the solar cycle phasing of geomagnetic storms.

The analysis consists of summing the number of storms for each calendar month and for each year. These distributions were also studied according to the storm peak intensities. For the latter effort, the following classification has been used: (a) $-75 < Dst_p \leq -50$; (b) $-100 < Dst_p \leq -75$; (c) $-100 < Dst_p \leq -50$; (d) $Dst_p \leq -100$; (e) $-200 < Dst_p \leq -100$; (f) $Dst_p \leq -150$; (g) $< Dst_p \leq -200$; (h) $< Dst_p \leq -250$.

3. Results

Fig. 2 shows the distribution of peak *Dst* (Dst_p) for all storms. The number of storms versus $-Dst_p$ is plotted. The average peak $-Dst_p$ is 94 nT and the median is 76 nT. Note that the number of storms follows roughly an exponential law, decreasing rapidly as the storm strength (negative intensity) increases. Therefore, an exponential decay function was fitted to the distribution, of the

form: $P(Dst_p) = P_o + Ae^{-Dst_p/t}$. From the fit results, one has the following empirical law for storms (in normalized occurrence):

(1) $P(Dst_p) = 0.0013 + 1.19e^{-Dst_p/34}$, or $P(Dst_p) \approx 1.2e^{-Dst_p/34}$ where Dst_p is given in nT.

In the top panel of Fig. 3 the number of storms with $Dst_p \leq -50$ nT per year are plotted with the yearly average sunspot number. The average and standard deviation of Dst_p for all storms during a given year is given in the bottom panel. The dual-peak distribution can be seen, with a peak around solar maximum and the other during the beginning of the declining phase. The solar maximum peak is often the greatest of the two peaks, but this is not found for all cycles. There is some relationship between the average Dst_p with sunspot number, but the standard deviations are very large, reflecting the wide range of storm intensities that occur every year.

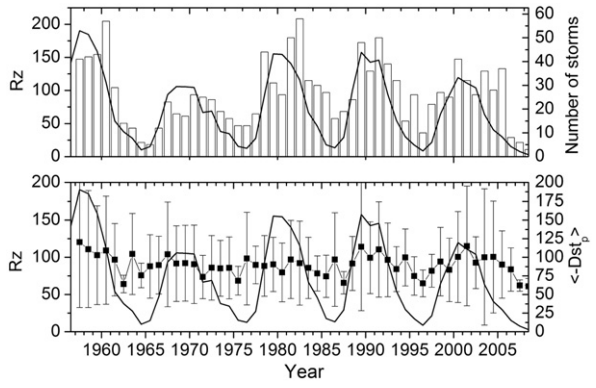

Fig. 3. Number of $Dst_p \leq -50$ nT storms per year (bars) and sunspot number annual averages (lines), top panel. The average of Dst_p and their statistical uncertainties (points and bars) and sunspot numbers (bottom panel) are indicated.

In Fig. 4, the levels of storm strength dependence on solar cycle are shown. The storm levels are labeled as discussed in the Method of Analysis session. From the Figure there is an indication that less intense storms have their peak occurrences in the declining phase, while more intense storms tend to have higher occurrence rates near solar maximum.

Fig. 5 shows the number of storms with $Dst_p \leq -50$ nT per calendar month of the year in the top panel, and average and standard deviation of peak Dst for all storms during a given month, in the bottom panel. A semi-annual variation can be clearly seen in the number of storms, with a peak around the equinoctial months, March through May and September through November. For the average Dst_p, it can be noted that, besides the semi-annual variation, there is a trend for high values of Dst_p to occur around July, with intensity similar to that of the equinoctial months.

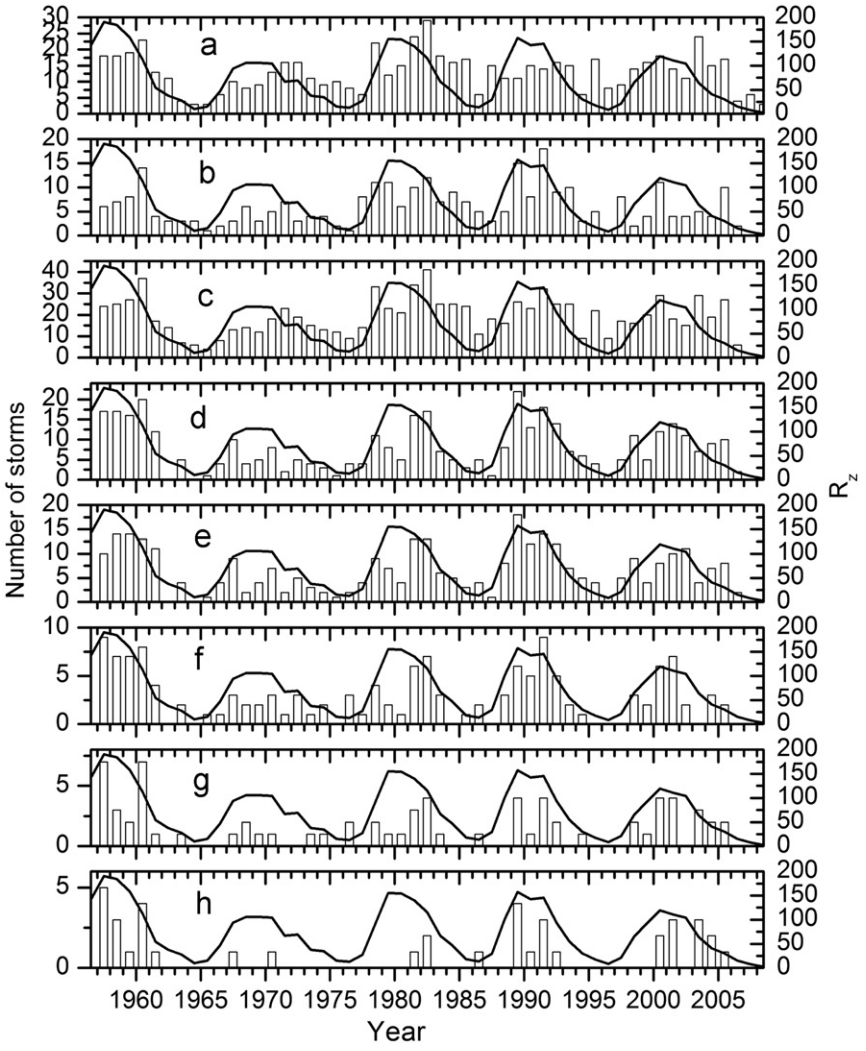

Fig. 4. The number of storms per year and sunspot number for different levels of storm strength: (a) $-75 < Dst_p \leq -50$; (b) $-100 < Dst_p \leq -75$; (c) $-100 < Dst_p \leq -50$; (d) $Dst_p \leq -100$; (e) $-200 < Dst_p \leq -100$; (f) $Dst_p \leq -150$; (g) $Dst_p \leq -200$; (h) $Dst_p \leq -250$.

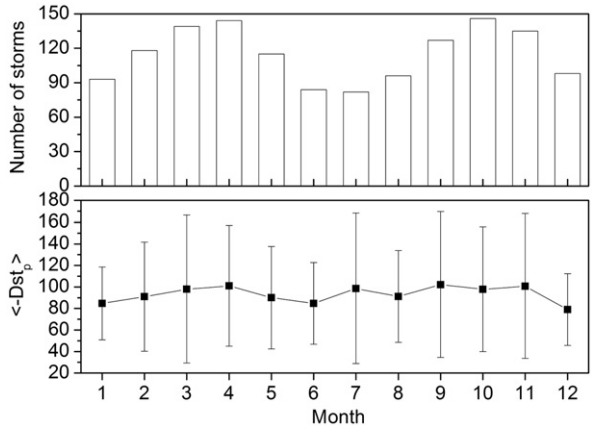

Fig. 5. The number of $Dst_p \leq -50$ nT storms per month of year (top panel). The averages and standard deviations of the Dst_p (bottom panel) are given.

Fig. 6 shows the distribution of storms per month of year for the same levels of storm strength as showed in Fig. 4. The semi-annual variation is observed for all storm strength levels. However, for more intense events, a peak in July is noticeable. The causes of this anomalous distribution have been tentatively attributed to: (1) seasonal variation in ionospheric conductivity (Clua de Gonzalez et al., 2001, 2002), (2) the interplanetary shock rate near the Earth's orbit being higher in July (Echer et al.,2005b) or (3) to solar "hot spots" regions (Bai, 1990; Echer et al., 2005b).

4. Conclusions

Using a newly derived list of geomagnetic storms with $Dst \leq -50$ nT for the 1957–2008 interval, the statistical distribution of solar cycle variation and annual/semi-annual variation of storms was analyzed. It is concluded that geomagnetic storms show a distribution that can be fitted by an exponential function.

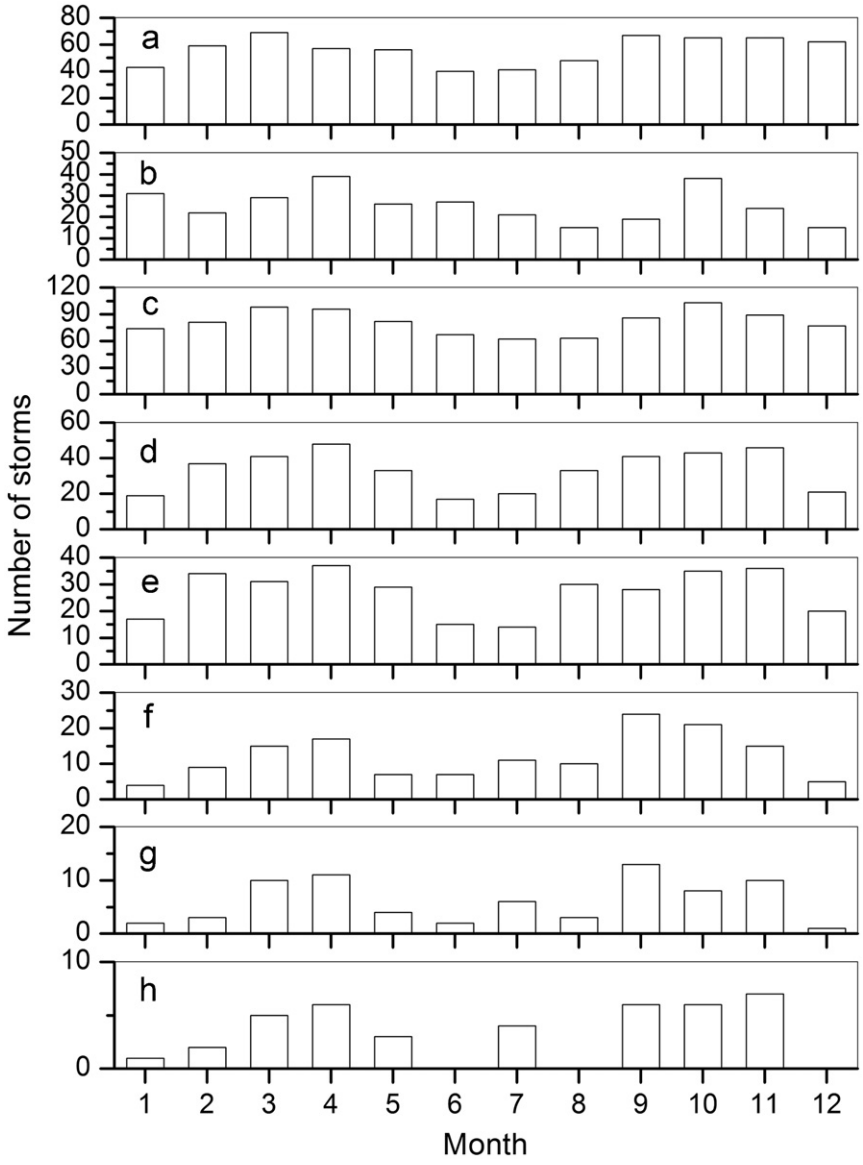

Fig. 6. Number of storms per month of year for different levels of storm strength: (a) $-75 < Dst_p \leq -50$; (b) $-100 < Dst_p \leq -75$; (c) $-100 < Dst_p \leq -50$; (d) $Dst_p \leq -100$; (e) $-200 < Dst_p \leq -100$; (f) $Dst_p \leq -150$; (g) $Dst_p \leq -200$; (h) $Dst_p \leq -250$.

The probability of having a storm with a given Dst_p is: $P(Dst_p) \sim 1.2e^{-Dst_p/34}$

This exponential distribution indicates that intense events have a much lower probability of occurrence than weaker storms. This result was not unexpected, especially since prior work (Tsurutani et al., 1990) has indicated that the interplanetary magnetic B_z field follows a Gaussian distribution. The fit that Tsurutani et al. (1990) obtained was $P(B_z) = Ae^{-B_z{}^2/28}$ where A is a constant. An obvious question is "can one use these distributions to predict the occurrence frequency of extreme events, such as the 1859 Carrington storm (Tsurutani et al., 2003)"? If one follows this logic, it can be noted that a storm of this intensity ($Dst_p = -1760$ nT) will have an almost null probability of $\sim 4 \times 10^{-23}$ (for comparison, a $Dst_p = -100$ nT storm will have a probability of 0.06). This is clearly incorrect. Tsurutani et al. (2003) have argued that one cannot use simple statistics to determine the probability of extreme storm occurrence. The high end tails of distribution functions do not have adequate statistics to make meaningful measurements. The physics associated with them may be different and therefore have different statistics as the 1859 storm and 1972 interplanetary event (Tsurutani et al., 1992) clearly show. Further research is needed on these "tail" events.

The solar cycle distribution of storms shows in general the dual peak variation, with a maximum occurrence around solar maximum and another in the post-maximum phase/declining phase. When studying storms according to their strength level, it was observed that less intense storms show a higher occurrence peak near the declining phase, while more intense storms show a higher occurrence close to solar maximum. The current hypothesis that stronger storms are caused by large active regions/CME activity in the solar maximum and early declining phase (e.g, Gonzalez et al., 2007; Tsurutani et al., 2008) and weaker storms are associated with CIRs in the declining phase (Tsurutani et al., 1995, 2006a,2006b; Gonzalez et al., 2007; Echer et al., 2008) seems to be borne out. However another possibility is that the sun may have two separate active phases for ICMEs and flares. An example for the latter is that in late 2003, well after sunspot maximum, there were the exceptionally intense Halloween flares/ICMEs (Mannucci et al., 2005; Tsurutani et al., 2005) and also strong high speed stream events (Tsurutani et al., 2011).

The semi-annual variation, with peak occurrence at the two equinoxes, is clearly noted for all intensity level storms. However the mechanism for these two peaks is currently under intense debate. Mursula et al. (2011) has clearly indicated that most years do not show a two-season profile in geomagnetic activity, but only one per year. The hypothesis of the Russell–McPherron coordinate transformation from GSE to GSM needs considerable further testing (Mursula and Zieger, 1996; Mursula et al., 2011).

For intense magnetic storms ($Dst_p < -100$ nT), an occurrence peak in July is apparent. Both the average peak Dst, and the occurrence of more intense storms, show a slight enhancement in July. This increase in occurrence has however only a modest effect on the monthly averaged Dst_p.

In conclusion, a new dataset of geomagnetic storms has been compiled, which should be useful for researchers of solar-terrestrial physics and space weather topics. The occurrence distribution of geomagnetic storms indicates a clear trend for geomagnetic storm intensities to follow an exponential distribution. Thus for storms of intensity $Dst_p > -300$ nT, occurrence frequency predictions should be applicable.

This unfortunately is not the case for the extreme events such as the 1859 Carrington storm and the extremely high speed solar wind event of August 1972. It was shown that by using the statistics presented here, the Carrington event would have been extremely rare. With the relative frequency of extreme events in the recent past (see the Table in Tsurutani et al., 2003), it is clear that the solar physics of these events are different from the less intense events discussed here. This topic should be a fruitful one for interested space plasma physicists.

Acknowledgments

EE would like to thank the CNPq (PQ-300211/2008-2) and FAPESP (2007/52533-1) agencies for financial support. WDG would like to thank FAPESP agency (2008/06650-9) for financial support. Portions of this work were performed at the Jet Propulsion Laboratory, California Institute of Technology under contract with NASA. BTT would like to thank INPE and his hosts for the hospitality during his sabbatical leave during 2010. We thank the World-Data Center for Geomagnetism—Kyoto for the Dst index data used in this study.

References

Akasofu, S.–I., 1981. Energy coupling between the solar wind and the magnetosphere. Space Sci. Rev. 28, 121–190.
Alves, M.V., Echer, E., Gonzalez, W.D., 2006. Geoeffectiveness of corotating interaction regions as measured by Dst index. J. Geophys. Res. 111, A07S05.
Bai, T., 1990. Solar "hot spots" are still hot. Astrophys. J. 364, L17–L20.
Baumjohann, W., 1986. Merits and limitations of the use of geomagnetic indices in solar wind-magnetosphere coupling studies. In: Kamide, Y., Slavin, J.A. (Eds.), Solar wind-magnetosphere coupling. Terra Scientific Publishing Co (TERRA-PUB), Tokyo, pp. 3–15.
Chapman, S., Bartels, J., 1940. Geomagnetism, vol. I. Oxford Univ. Press, New York.
Clua de Gonzalez, A.L., Silbergleit, V.M., Gonzalez, W.D., Tsurutani, B.T., 2001. Annual variation of geomagnetic activity, J. Atmos. Sol. Terr. Phys. 63, 367–374.
Clua de Gonzalez, A.L., Silbergleit, V.M., Gonzalez, W.D., Tsurutani, B.T., 2002. Irregularities in the semiannual variation of the geomagnetic activity. Adv. Space Res. 30, 2215–2218.
Daglis, I.A., Thorne, R.M., 1999. The terrestrial ring current: origin, formation, and decay. Rev. Geophys. 37, 407–438.
Dessler, A.J., Parker, E., 1959. Hydromagnetic theory of magnetic storms. J. Geophys. Res. 64, 2239–2259.
Dungey, J.W., 1961. Interplanetary magnetic field and the auroral zones. Phys. Rev. Lett. 6, 47–48.
Echer, E., Gonzalez, W.D., 2004. Geoeffectiveness of interplanetary shocks, magnetic clouds, sector boundary crossings and their combined occurrence. Geophys. Res. Lett. 31, L09808 doi:10.1029/2003GL019199.
Echer, E., Gonzalez, W.D., Guarnieri, F.L., Dal Lago, A., Schuch, N.J., 2005a. Introduction to Space Weather. Adv. Space Res. 35, 855–865.
Echer, E., Gonzalez, W.D., Tsurutani, B.T., Vieira, L.E.A., Alves, M.V., Gonzalez, A.L.C., 2005b. On the preferential occurrence of interplanetary shocks in July and November: causes (solar wind annual dependence) and consequences (intense magnetic storms). J. Geophys. Res. 110, A02101 doi:10.1029/2004JA010527.
Echer, E., Gonzalez, W.D., Alves, M.V., 2006. On the geomagnetic effects of solar wind interplanetary magnetic structures. Space Weather 4, S06001 doi:10.1029/2005SW000200.
Echer, E., Gonzalez, W.D., Tsurutani, B.T., Gonzalez, A.L.C., 2008. Interplanetary conditions causing intense geomagnetic storms ($Dst \leq -100$ nT) during solar cycle 23 (1996-2006). J. Geophys. Res. 113, A05221 doi:10.1029/2007JA012744.
Feldstein, Y.I., et al., 1990. Magnetic field of the magnetospheric ring current and its dynamics during magnetic storms, J. Atmos. Solar-Terr. Phys. 52, 1185–1191.
Feldstein, Y.I., Dremukhina, L.A., Levitin, A.E., Mall, U., Alexeev, I.I., Kalegaev, V.V., 2003. Energetics of the magnetosphere during the magnetic storm, J. Atmos. Solar-Terr. Phys. 65, 429–446.
Fok, M.C., et al., 1995. 3-D dimensional ring current decay model. J. Geophys. Res. 100, 9619–9632.
Gonzalez, W.D., Mozer, F.S., 1974. A quantitative model for the potential resulting from reconnection with an arbitrary interplanetary magnetic field. J. Geophys. Res. 79, 4186.
Gonzalez, W.D., Tsurutani, B.T., 1987. Criteria of interplanetary parameters causing intense magnetic storms ($Dst < -100$ nT). Planet. Space Sci. 35, 1101.
Gonzalez, W.D., Gonzalez, A.L.C., Tsurutani, B.T., 1990. Dual-peak solar cycle distribution of intense geomagnetic storms. Planet. Space Sci. 38, 181–187.
Gonzalez, W.D., Joselyn, J.A., Kamide, Y., Kroehl, H.W., Rostoker, G., Tsurutani, B.T., Vasyliunas, V., 1994. What is a geomagnetic storm. J. Geophys. Res. 99, 5771–5792.
Gonzalez, W.D., Tsurutani, B.T., Clua de Gonzalez, A.L., 1999. Interplanetary origin of geomagnetic storms. Space Sci. Rev. 88, 529–562.
Gonzalez, W.D., Echer, E., 2005. A study on the peak Dst and peak negative Bz relationship during intense geomagnetic storms. Geophys. Res. Lett. 32, L18103 doi:10.1029/2005GL023486.

Gonzalez, W.D., Echer, E., Clua-Gonzalez, A.L., Tsurutani, B.T., 2007. Interplanetary origin of intense geomagnetic storms (Dst < -100 nT) during solar cycle 23. Geophys. Res. Lett. 34, L06101 doi:10.1029/2006GL028879.

Guarnieri, F.L., Tsurutani, B.T., Gonzalez, W.D., Echer, E., Gonzalez, A.L., Grande, M., Soraas, F., 2006. ICME and CIR storms with particular emphasis on HILDCAA events. In: Proceedings of ILWS Workshop.

Hirshberg, J., Colburn, D.S., 1969. Interplanetary field and geomagnetic variations, a unified view. Planet. Space Sci. 17, 1183–1206.

Humboldt, A. von, 1808. Die vollständigeste aller bisherigen Beobachtungen über den Einfluss des Nordlichtes auf die Magnetnadel. Gilb. Ann., 29.

Kozyra, J.U., Jordanova, V.K., Horne, R.B., Thorne, R.M., 1997. Modelling of the contribution of electromagnetic ion cyclotron (EMIC) waves to storm-time ring current erosion. In: Tsurutani, B.T., Gonzalez, W.D., Kamide, Y., Arballo, J.K. (Eds.), Magnetic Storms, Geophysical Monograph 98. American Geophysical Union 187-202.

Mannucci, A.J., Tsurutani, B.T., Iijima, B.A., Komjathy, A., Saito, A., Gonzalez, W.D., Guarnieri, F.L., Kozyra, J.U., Skoug, R., 2005. Dayside global ionospheric response to the major interplanetary events of October 29–30, 2003 ''Halloween storms''. Geophys. Res. Lett. 32 (L12S02). doi:10.1029/2004GL021467.

Mursula, K., Zieger, B., 1996. The 13.5-day periodicity in the Sun, solar wind and geomagnetic activity: the last three solar cycles. J. Geophys. Res. 101, 27077–27090.

Mursula, K., Tanskane, E., Love, J.J., 2011. Spring-Fall asymmetry of substorm strength, geomagnetic activity and solar wind: implications for semiannual variation and solar hemispheric asymmetry. Geophys. Res. Lett. 38, L06104 doi:10.1029/2011GL046751.

Priester, W., Catanni, D., 1962. On the semiannual variations of geomagnetic activity and its relations to the solar corpuscular radiation. J. Atmos. Sci. 19, 121–126.

Rostoker, G., 1972. Geomagnetic indexes. Rev. Geophys. Space Phys. 10, 935–950.

Rostoker, G., Falthammar, C.G., 1967. Relationship between changes in the interplanetary magnetic field and variations in the magnetic field at Earth's surface. J. Geophys. Res. 72, 5853.

Russell, C.T., McPherron, R.L., 1973. Semiannual variation of geomagnetic activity. J. Geophys. Res. 78, 92–108.

Sckopke, N., 1966. A general relation between energy of trapped particles and disturbance field near earth. J. Geophys. Res. 71, 3125.

Sorras, F., et al., 2004. Evidence for particle injection as the cause of Dst reduction during HILDCAA events,. J. Atmos. Solar-Terr. Phys 66, 177–186.

Sugiura, M., 1964. Hourly values of equatorial Dst for the IGY. Annual International Geophysical Year, vol. 35. Pergamon, New York, p. 9.

Tsurutani, B.T., Gonzalez, W.D., 1987. The cause of high-intensity long-duration continuous AE activity (HILDCAAs) interplanetary Alfven wave trains, Planet. Space Sci 35, 405–412.

Tsurutani, B.T., et al., 1988. Origin of interplanetary southward magnetic fields responsible for major magnetic storms near solar maximum (1978-1979). J. Geophys. Res 93, 8519.

Tsurutani, B.T.T., Gould, B.E., Goldstein, W.D., Gonzalez, Sugiura, M., 1990. Interplanetary Alfven waves and auroral (substorm) activity: IMP 8. J. Geophys. Res. 98 (A3), 2241–2252.

Tsurutani, B.T., Gonzalez, W.D., Tang, F., Lee, Y.T., Okada, M., 1992. Reply to L.J. Lanzerotti: solar wind ram pressure convection estimation of the efficiency of viscous interaction. Geophys. Res. Lett. 19, 1993–1996.

Tsurutani, B.T. et al., 1995. Interplanetary origin of geomagnetic activity in the declining phase of the solar cycle, J. Geophys. Res., 100, 21,717.

Tsurutani, B.T., et al., 1997. Preface, AGU Geophys. Monogr. 98, Magn.Storms, ix–x.

Tsurutani, B.T., et al., 2003. The extreme magnetic storm of. J. Geophys. Res. 108, 1268 doi:10.1029/2002JA009504.

Tsurutani, B.T., D.L. Judge, F.L. Guarnieri, P. Gangopadhyay, A.R. Jones, J. Nuttall, G.A. Zambon, L. Didkovsky, A.J. Mannucci, B. Iijima, R.R. Meier, T.L. Immel, T.N. Woods, S. Prasad, L. Floyd, J. Huba, S.C. Solomon, P. Straus and R. Viereck, 2005. The October 28, 2003 extreme EUV solar flare and resultant extreme ionospheric effects: Comparison to other Halloween events and the Bastille Day event, Geophys. Res. Lett., 32, L03S09, doi:10.1029/2004GL021475.

Tsurutani, B.T., et al., 2006a. Corotating solar wind streams and recurrent geomagnetic activity: a review,. J. Geophys. Res. 111, A07S01 doi:10.1029/2005JA011273.

Tsurutani, B.T., et al., 2006b. Magnetic storms caused by corotating solar wind streams, in Recurrent Magnetic Storms: Corotating Solar Wind Streams, edited by B.T. Tsurutani, R.L. McPherron, W.D. Gonzalez, G. Lu, J.H.A. Sobral and N. Gopalswamy, Amer. Geophys. U. Monograph, Wash. D.C., 167, 1.

Tsurutani, B.T., Echer, E., Guarnieri, F.L., Verkhoglyadova, O.P., 2008. Interplanetary causes of middle latitude ionospheric disturbances. In: Kintner Jr., P., Coster, A.J., Fuller-Rowell, T., Manucci, A.J., Mendillo, M., Heelis., R. (Eds.), (Org.). Midlatitude Ionospheric Dynamics and Disturbances Geophysical Monograph Series. American Geophysical Union 99-120.

Tsurutani, B.T., E..Echer, F.L. Guarnieri and W.D. Gonzalez, 2011. The properties of two solar wind high speed streams and related geomagnetic activity during the declining phase of solar cycle 23, J. Atmos. Sol.-Terr. Phys., doi:10.1016/j.jastp.2010.04.003.